Two-photon spectroscopy of the francium $8S_{1/2}$ level

J. E. Simsarian, W. Z. Zhao, L. A. Orozco, and G. D. Sprouse
Department of Physics and Astronomy, State University of New York at Stony Brook, Stony Brook, New York 11794-3800
(Received 11 May 1998)

We report the spectroscopy of the $8S_{1/2}$ energy level in ^{210}Fr by two-photon excitation of atoms confined and cooled in a magneto-optical trap. The resonant intermediate level is the upper state of either the $7P_{3/2}$ trapping transition or the $7P_{1/2}$ repumping transition. The center-of-gravity energy difference between the $7S_{1/2}$ ground level and the $8S_{1/2}$ level is $19\,732.523 \pm 0.004$ cm^{-1}. The hyperfine separation of the $8S_{1/2}$, $F=11/2$ and $F=13/2$ states is $10\,256 \pm 7$ MHz, giving a magnetic dipole hyperfine constant A of 1577.8 ± 1.1 MHz. [S1050-2947(99)01201-9]

PACS number(s): 32.30.−r, 32.10.Fn, 31.30.Gs

Francium has the simplest electronic structure of the heavy elements but has no stable isotopes. Spectroscopic measurements of the Fr atomic structure test *ab initio* calculations that predict energy levels and hyperfine splittings [1–4]. In particular, the hyperfine structure is sensitive to relativistic, core polarization, and core correlation effects that are difficult to calculate accurately in multielectron atoms. A further motivation for its study is the possibility of performing spectroscopic measurements that test fundamental symmetries in Fr.

While the atomic structure of most alkali-metal atoms has been extensively studied, there is no similar knowledge for Fr. Many levels and hyperfine splittings were located in the experiments at ISOLDE [5] and with a natural source [6]. It is now possible to study francium in an ideal environment for spectroscopy: a magneto-optical trap on-line with an accelerator that produces it [7] or with a natural source [8]. Recently measured atomic properties include the location of the $9S_{1/2}$ level [9], the lifetimes of the $7P_{3/2}$ and $7P_{1/2}$ levels [10,11] and accurate measurements of the hyperfine splittings of the $7p$ levels [8].

A better understanding of the complex francium atom is an important test for the atomic structure calculations [12,13] needed to extract weak force parameters from recent atomic parity nonconservation (PNC) experiments in Cs [14]. For a review of the current theoretical methods employed in the calculations see Ref. [15]. The ability to calculate the hyperfine constants implies accurate wave functions at short radius, the same region where the weak interaction occurs. The hyperfine interaction also gives information about nuclear structure; for example, the hyperfine anomaly (Bohr-Weisskopf effect) probes the nuclear magnetization and its variations in a chain of isotopes. It is sensitive to changes in the radial distribution of the neutron magnetization.

In this paper we present our measurements of the $7S_{1/2} \rightarrow 8S_{1/2}$ energy interval and hyperfine splitting of the $8S_{1/2}$ level by resonant two-photon spectroscopy. The dipole-forbidden $7S_{1/2} \rightarrow 8S_{1/2}$ transition is a candidate for a PNC experiment in Fr and the $8S_{1/2}$ level had not been previously located.

To make Fr, a beam from the Stony Brook superconducting linear accelerator impinges on a Au target producing in it $\approx 1 \times 10^6$/s ^{210}Fr, which has a half-life of 3.2 min. We separate the production and trapping regions by extracting the francium atoms out of the gold as ions and transport them about 1 m, where they are neutralized on a heated yttrium surface. The neutral atoms are released into a nonstick dry-film coated glass cell where the magneto-optical trap (MOT) forms. The physical trap consists of a 10-cm-diam Pyrex bulb with six 5-cm-diam windows and two viewing windows 3 cm in diameter. The MOT is formed by six intersecting laser beams each with 7.8-mW/cm^2 intensity and a magnetic field gradient of 6 G/cm. The $1/e$ fill time of the trap is 20 s.

The trap operates on-line in the target room of the accelerator and we remotely control the experiment. Before trapping Fr, the apparatus is tested extensively with stable Rb. The Rb comes from a dispenser next to the Au target and follows the same path through the apparatus as the Fr. We use the trapped Rb to test the excitation and detection schemes needed for the Fr measurements. We have studied the hyperfine splitting of the $6S_{1/2}$ level of ^{85}Rb to test the method we apply to Fr.

Figure 1 shows the energy levels of the ^{210}Fr atom relevant for trapping and for the two-photon spectroscopy. A Coherent 899-21 titanium-sapphire laser excites the trapping and cooling transition $7S_{1/2}$, $F=13/2 \rightarrow 7P_{3/2}$, $F=15/2$ at 718 nm. We frequency modulate the trapping laser at 15 kHz and use lock-in techniques to detect the trap fluorescence. An 817-nm EOSI 2010 diode laser returns any atoms that leak out of the cooling cycle via the $7S_{1/2}$, $F=11/2 \rightarrow 7P_{1/2}$, $F=13/2$ transition.

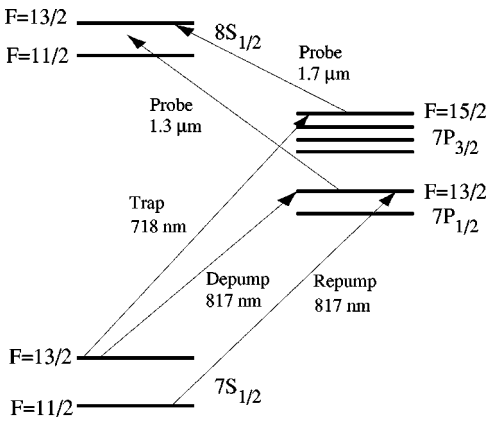

FIG. 1. Diagram of energy levels of ^{210}Fr relevant for trapping and two-photon excitation.

 ©1999 The American Physical Society

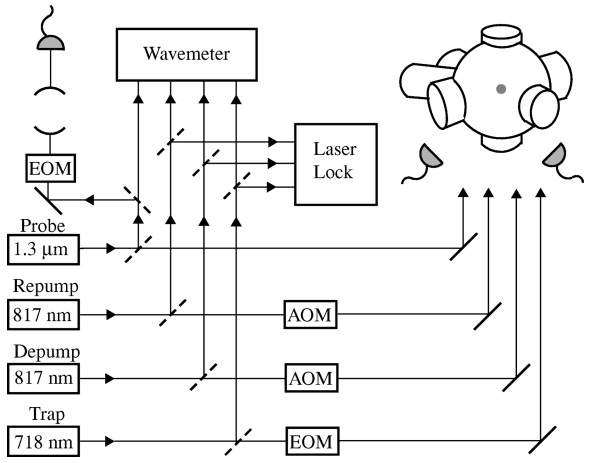

FIG. 2. Diagram of the experimental setup for 1.3-μm excitation.

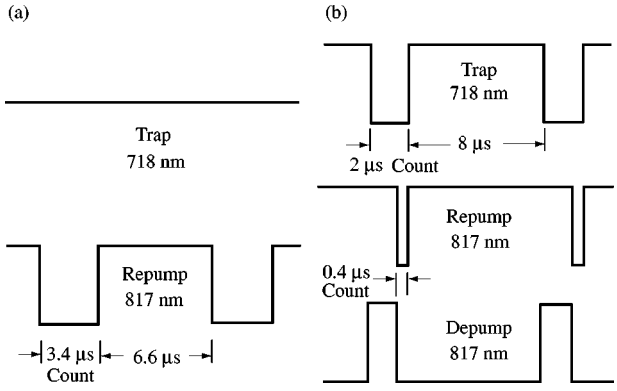

FIG. 3. (a) Time sequence for two-photon excitation with the 1.7-μm laser. (b) Time sequence for two-photon excitation with the 1.3-μm laser.

We use two different levels, $7P_{3/2}$ or $7P_{1/2}$, for the first step to the $8S_{1/2}$ level (see Fig. 1). Only the $8S_{1/2}$, $F=13/2$ level can be reached with an electric dipole-allowed transition when the $7P_{3/2}$, $F=15/2$ level is the intermediate state. An EOSI 2001 diode laser ($In_xGa_{1-x}As/InP$) operating at 1.7 μm with a linewidth of 110 MHz full width at half maximum (FWHM) excites this transition. Both of the $8S_{1/2}$ hyperfine states can be reached when the $7P_{1/2}$, $F=13/2$ level is the intermediate state. An EOSI 2010 diode laser operating at 1.3 μm with a linewidth of 30 MHz FWHM excites this transition. We achieve long-term frequency stability of all the lasers except for the probe by sending part of the beams into a Fabry-Pérot cavity along with a frequency-stabilized He-Ne laser. A digital feedback loop locks the lasers to the stabilized He-Ne with less than ± 1 MHz/h drift [16]. A Burleigh WA-1500 wavemeter measures the frequencies of the lasers (see Fig. 2).

To locate the trap, we set the lasers close to the resonances and then scan the trapping and repumping laser frequencies while looking for 718-nm florescence detected with the lock-in amplifier or a charge-coupled-device camera. Once the trap is established, the nuclear fusion reaction products continuously replenish the sample of atoms and the digital frequency lock maintains the lasers on resonance. The 718-nm trap fluorescence remains stable for hours.

The *ab initio* calculations by Dzuba *et al.* [1] and Johnson [2] of the ionization energy of the $8S_{1/2}$ state have an expected accuracy of a few fractions of a percent. A search of 0.1% or 20 cm^{-1} is difficult, so we use a quantum-defect fit as a guide. The calculation includes the Fr $10S_{1/2}$ to $22S_{1/2}$ levels and ionization potential from ISOLDE [5] and our measurement of the $9S_{1/2}$ level [9]. The interpolation narrowed the search to a window of less than 1 cm^{-1}.

To excite the atoms from the $7P_{3/2}$ level, we split the 1.7-μm laser beam and send part to the wavemeter and the rest to the trap. The atoms decay from the $8S_{1/2}$ to the ground state through the $7P_{1/2}$ and $7P_{3/2}$ levels and we detect the fluorescence from the $7P_{1/2}$ level at 817 nm. Since the repumping laser contributes background scattered light at 817 nm, an acousto-optic modulator (AOM) extinguishes the light while a Hamamatsu 636-10 photomultiplier tube (PMT) detects the fluorescence in photon-counting mode [see Fig. 3(a) for the time cycle]. Appropriate interference filters reject light other than at 817 nm. We shape and amplify the pulses and send them to a gated scaler that counts photons when the repumping laser is off. The timing signals come from a digital gate generator (Stanford Research DS400). A computer controls the lasers and reads the wavemeter and the 817-nm scaler. When the 1.7-μm laser excites the $7P_{3/2},F=15/2 \rightarrow 8S_{1/2},F=13/2$ transition, the 817-nm scalar counts increase and the 718-nm fluorescence decreases accompanied by a change in the shape of the cloud of atoms.

Figure 2 is a schematic diagram of the apparatus used for the excitation from the $7P_{1/2}$ level. Two lasers excite the atoms to the intermediate state from each of the hyperfine ground states (see Figs. 1 and 2). The 817-nm EOSI 2010 repumping laser excites atoms from the $7S_{1/2},F=11/2$ state and a titanium sapphire depumping laser excites atoms from the $7S_{1/2},F=13/2$ state. To ensure that both lasers are on resonance AOMs extinguish them simultaneously and a PMT and photon counting electronics detect the fluorescence of the $7P_{1/2}$ level. We adjust the laser frequencies to maximize the 817-nm fluorescence. A second Hamamatsu 636-10 PMT detects 718-nm photons from the decay cascade of the $8S_{1/2}$ level. Two cascaded Gsänger LM0202 electro-optic modulators (EOMs) extinguish the trapping light during the photon counting to reduce the background light [see Fig. 3(b) for the time cycle]. The computer scans the 1.3-μm laser at a rate of 0.7 MHz/s in the increasing and decreasing frequency directions and records the $8S_{1/2}$ resonance in the 718-nm photon counts. We send part of the 1.3-μm laser through an EOM that provides 100-MHz sidebands before it enters a 300-MHz free spectral range, temperature-stabilized Fabry-Perot cavity (≈ 8 MHz/h drift) that provides a frequency reference. Figure 4 shows resonances of the $8S_{1/2},F=13/2$ and $F=11/2$ hyperfine states together with the étalon signal with the 100-MHz frequency markers.

The probe laser bandwidth determines the resonance widths since the cold atoms have negligible Doppler broadening. The long-term linewidth of the laser is broad. Acoustic noise from the target area couples to the laser producing a linewidth of about 30 MHz over a few seconds. The noise has long-period oscillations that contribute to the broadening and asymmetries observed in Fig. 4. During a scan we monitor the laser with a Fabry-Perot cavity, but we have not been able to obtain a unique deconvolution of the atomic line

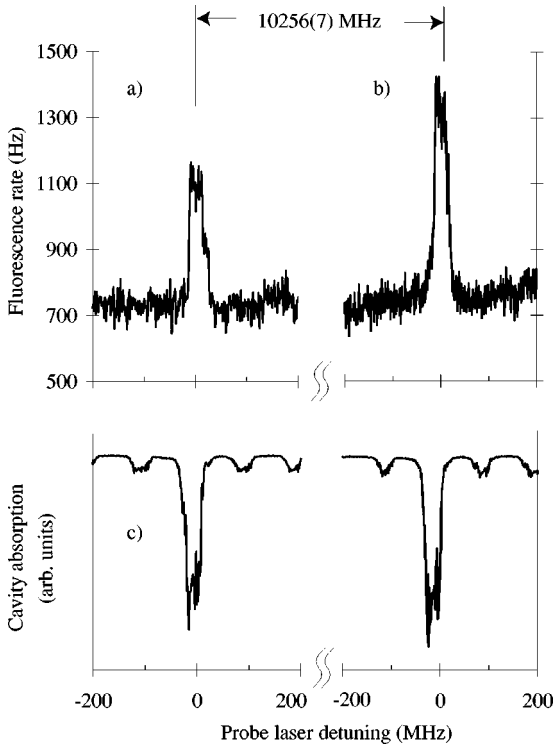

FIG. 4. (a) Fluorescence at 718 nm from excitation to the $8S_{1/2}$, $F=11/2$ state vs the 1.3-μm laser frequency detuning. The zero of the scan corresponds to 7494.757 ± 0.003 cm^{-1}. (b) Fluorescence from the $8S_{1/2}$, $F=13/2$ state vs the 1.3-μm laser frequency detuning. (c) Etalon signals with 100-MHz markers.

shape due to uncertainties in the parameters of the cavity and its alignment. We have performed off-line a series of measurements of the linewidth of the laser using a Fabry-Perot cavity. With the laser subjected to similar noise conditions to those present in the target area, we have found the center of gravity of the cavity resonances to be accurate to better than 1 MHz. We do not observe the Autler-Townes splitting of the intermediate level because the intensities of the 817-nm lasers are low. The size of the trap is less than 1 mm in diameter and resides in a magnetic field gradient of 6 G/cm. The largest splitting in the magnetic manifold is less than the 30-MHz linewidth of the probe laser.

We determine the center of gravity of the $7S_{1/2}\rightarrow8S_{1/2}$ transition and hyperfine splitting from the recorded wavemeter readings and resonances. To test the absolute performance of our wavemeter we reproduced the absolute calibration of the D_2 ^{87}Rb line [17] and the D_2 ^{133}Cs line [18] within ±0.001 cm^{-1}, as well as the molecular iodine lines 380, 381, and 382 [19], which had an average deviation of 0.003 cm^{-1}. Based on these calibrations, we assign ±0.003 cm^{-1} as the accuracy of the wavemeter.

The measurements using the $7P_{1/2}$ and $7P_{3/2}$ as intermediate levels give independent determinations of the $7S_{1/2}\rightarrow8S_{1/2}$ transition energy. We add the wave numbers of the two photons, one from the trapping or repumping laser and the other from the probe laser to obtain the transition energy. We use our measurement of the hyperfine splitting of the $8S_{1/2}$ and the measured $7S_{1/2}$ ground-state magnetic dipole hyperfine constant $A(7195.1\pm0.4$ MHz) [20] to find the center of gravity of the transition. The repeatability of the francium resonance for increasing and decreasing frequency scans is better than 0.001 cm^{-1}. The difference in the $7S_{1/2}\rightarrow8S_{1/2}$ transition energy between the two excitation paths is consistent with zero. We add in quadrature the accuracy of the wavemeter (±0.003 cm^{-1}), the uncertainty for the first step photon (±0.002 cm^{-1}), and the uncertainty for the second step photon (±0.002 cm^{-1}) to obtain a total uncertainty of ±0.004 cm^{-1}. The center-of-gravity energy interval between the $7S_{1/2}\rightarrow8S_{1/2}$ levels of ^{210}Fr is $19\,732.523\pm0.004$ cm^{-1}.

TABLE I. Fitted quantum-defect parameters for the $nS_{1/2}$ series of francium.

Reference	δ_0	δ_2	δ_4	δ_6
[5]	5.07063(4)	0.282(2)	0.191(4)	
[5]	5.07073(7)	0.276(4)	0.28(6)	
this work	5.070711(9)	0.2765(3)	0.300(3)	-0.302(5)

The *ab initio* calculations use many-body perturbation theory to calculate the ionization energy of the $8S_{1/2}$ level. We use the ionization energy of the $7S_{1/2}$ level from Ref. [5] to compare our result with the calculations of Dzuba *et al.* (19 739 cm^{-1}) [1] and Johnson (19 665 cm^{-1}) [2]. Their predictions agree with our measurement to better than 4 parts in 10^3.

The $8S_{1/2}$ level completes the lower part of $nS_{1/2}$ series of francium. The energies of the $nS_{1/2}$ levels are well represented by the Rydberg series

$$E_{nS}=E_{\rm ion}-\frac{R_m}{n_{\rm eff}^2}, \tag{1}$$

where $E_{\rm ion}$ is the ionization energy of the ground state, E_{nS} is the energy of the $nS_{1/2}$ level measured from the ground state, and R_m is the reduced mass Rydberg constant. Equation (1) assigns an effective quantum number $n_{\rm eff}$ to the known francium $nS_{1/2}$ levels. We use an iterative algorithm to fit the quantum defect parameters δ_0, δ_2, δ_4, and δ_6 to the measured energies using

$$n_{\rm eff}=n-\delta$$
$$=n-\left(\delta_0+\frac{\delta_2}{(n-\delta)^2}+\frac{\delta_4}{(n-\delta)^4}+\frac{\delta_6}{(n-\delta)^6}+\cdots\right), \tag{2}$$

where δ is the quantum defect. Table I gives the quantum-defect parameters from three fits: rows 1 and 2 by Arnold *et al.* [5] and 3 from this work. Row 1 includes the $7S_{1/2}$ and $10S_{1/2}$-$22S_{1/2}$ levels. Row 2 includes the $10S_{1/2}$-$22S_{1/2}$ levels. Row 3 includes the $7S_{1/2}$-$22S_{1/2}$ levels. Figure 5 compares the measured energy levels of the $nS_{1/2}$ series to our quantum-defect calculation. We correct for the isotope and hyperfine shifts from ^{210}Fr to ^{212}Fr to use the measurements of Arnold *et al.* [5] in our fit.

We obtain the $8S_{1/2}$, $F=11/2$ to $F=13/2$ hyperfine splitting from the wavemeter readings of the resonances with the $7P_{1/2}$ as the intermediate level. We use the center of gravity of the line from the wavemeter readings and assign an un-

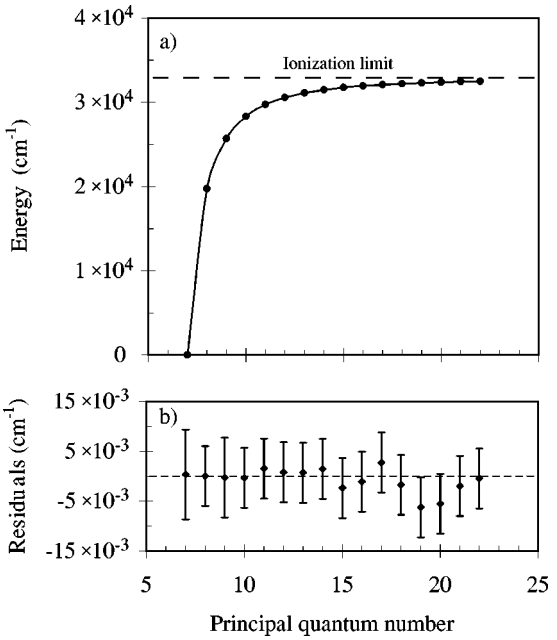

FIG. 5. (a) Quantum defect fit to the S series of francium using data from Refs. [5,9] and the present work. (b) Residuals of a four-parameter quantum-defect fit.

certainty of ± 7 MHz. We have checked the accuracy of this method by measuring other hyperfine splittings using simultaneously the wavemeter and rf techniques. Another way to get the hyperfine splitting is to employ those cavity markers. However, to compete with the wavemeter method, we have to know the free spectral range of our cavity to an accuracy better than 0.2 MHz. Due to the uncertainties of the peak positions, the nonlinearity of the laser scan, and the thermal drift of the cavity, we are not in a position to get a more accurate result this way with the available data. Figure 6 compares our measurement of the ^{210}Fr $8S_{1/2}$ magnetic hyperfine A constant to the predictions by Dzuba *et al.* [3], which, according to the authors, have an accuracy not worse

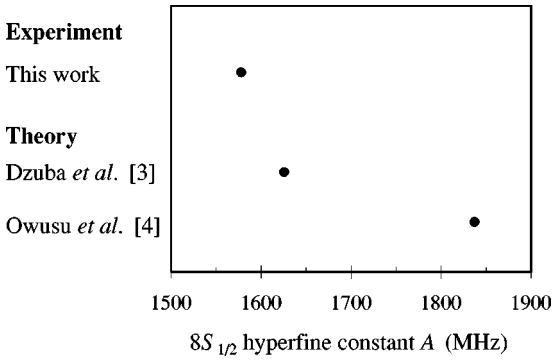

FIG. 6. Comparison of the measured magnetic dipole hyperfine constant A of the $8S_{1/2}$ level with *ab initio* predictions from Refs. [3,4]. The experimental error is smaller than the size of the dot.

than 3%, and Owusu *et al.* [4]. We use the measurements of the magnetic moments of Ref. [21] and the nuclear spins to obtain a hyperfine constant A for ^{210}Fr from the theoretical calculations. The hyperfine separation of the $8S_{1/2}$ level of ^{210}Fr is $10\,256 \pm 7$ MHz, which gives a hyperfine constant A of 1577.8 ± 1.1 MHz with an overall fractional accuracy in the A hyperfine constant of 7×10^{-4}.

We have performed two-photon spectroscopy of francium in a MOT using the $7p$ levels as intermediate resonant steps to measure the energy interval between the $7S_{1/2}$ and $8S_{1/2}$ levels. The location of the $8S_{1/2}$ level is necessary for the continuing effort to study parity nonconservation in francium. We have also measured the hyperfine splitting of the $8S_{1/2}$ level of ^{210}Fr and compared the result with *ab initio* calculations. Measurements of the same hyperfine splitting in other isotopes could reveal nuclear structure information that can be sensitive to changes in the neutron distribution.

We thank S. Christe for help in the characterization of the 1.3-μm laser. This work was supported in part by a Precision Measurement Grant from NIST and by NSF.

[1] V. A. Dzuba, V. V. Flambaum, and O. P. Sushkov, Phys. Rev. A **51**, 3454 (1995).
[2] W. R. Johnson (private communication).
[3] V. A. Dzuba, V. V. Flambaum, and O. P. Sushkov, J. Phys. B **17**, 1953 (1984).
[4] A. Owusu, R. W. Dougherty, G. Gowri, T. P. Das, and J. Andriessen, Phys. Rev. A **56**, 305 (1997); T. P. Das (private communication).
[5] E. Arnold, W. Borchers, H. T. Duong, P. Juncar, J. Lermé, P. Lievens, W. Neu, R. Neugart, M. Pellarin, J. Pinard, J. L. Vialle, K. Wendt, and the ISOLDE Collaboration, J. Phys. B **23**, 3511 (1990).
[6] S. V. Andreev, V. I. Mishin, and V. S. Letokhov, J. Opt. Soc. Am. B **5**, 2190 (1988).
[7] J. E. Simsarian, A. Ghosh, G. Gwinner, L. A. Orozco, G. D. Sprouse, and P. A. Voytas, Phys. Rev. Lett. **76**, 3522 (1996).
[8] Z.-T. Lu, K. L. Corwin, K. R. Vogel, C. E. Wieman, T. P. Dinneen, J. Maddi, and H. Gould, Phys. Rev. Lett. **79**, 994 (1997).
[9] J. E. Simsarian, W. Shi, L. A. Orozco, G. D. Sprouse, and W. Z. Zhao, Opt. Lett. **21**, 1939 (1996).
[10] W. Z. Zhao, J. E. Simsarian, L. A. Orozco, W. Shi, and G. D. Sprouse, Phys. Rev. Lett. **78**, 4169 (1997).
[11] J. E. Simsarian, L. A. Orozco, G. D. Sprouse, and W. Z. Zhao, Phys. Rev. A **57**, 2448 (1998).
[12] V. A. Dzuba, V. V. Flambaum, and O. P. Sushkov, Phys. Rev. A **56**, R4357 (1997).
[13] S. A. Blundell, W. R. Johnson, and J. Sapirstein, Phys. Rev. Lett. **65**, 1411 (1990); Phys. Rev. D **45**, 1602 (1992).
[14] C. S. Wood, S. C. Bennett, D. Cho, B. P. Masterson, J. L. Roberts, C. E. Tanner, and C. E. Wieman, Science **275**, 1759 (1997).
[15] J. Sapirstein, Rev. Mod. Phys. **70**, 55 (1998).
[16] W. Z. Zhao, J. E. Simsarian, L. A. Orozco, and G. D. Sprouse, Rev. Sci. Instrum. (to be published).
[17] J. Ye, S. Swartz, P. Jungner, and J. L. Hall, Opt. Lett. **21**, 1280 (1996).

[18] G. Avila, P. Gain, E. De Clercq, and P. Cerez, Metrologia **22**, 111 (1986).

[19] S. Gesternkorn, J. Vergès, and J. Chevillard, *Atlas du Spectre D'Absorption de la Molécule d'Iode 10 000-14 000 cm^{-1}* (Editions du Centre National de la Recherche Scientifique, Paris, 1978), Pt. I.

[20] A. Coc, C. Thibault, F. Touchard, H. T. Duong, P. Juncar, S. Liberman, J. Pinard, J. Lermé, J. L. Vialle, S. Büttgenbach, A. C. Mueller, A. Pesnelle, and the ISOLDE Collaboration, Phys. Lett. **163B**, 66 (1985).

[21] C. Ekström, L. Robertsson, and A. Rosén, Phys. Scr. **34**, 624 (1986).